*Journal of Physiology*

# Molecular mechanism of a COOH-terminal gating determinant in the ROMK channel revealed by a Bartter's disease mutation

Thomas P. Flagg *, Dana Yoo *, Christopher M. Sciortino†, Margaret Tate, Michael F. Romero †
and Paul A. Welling

*Department of Physiology, University of Maryland School of Medicine, Baltimore, MD 21201 and †Department of Physiology & Biophysics, Case Western Reserve University School of Medicine, Cleveland, OH 44106, USA*

The ROMK subtypes of inward-rectifier $K^+$ channels mediate potassium secretion and regulate NaCl reabsorption in the kidney. Loss-of-function mutations in this pH-sensitive $K^+$ channel cause Bartter's disease, a familial salt wasting nephropathy. One disease-causing mutation truncates the extreme COOH-terminus and induces a closed gating conformation. Here we identify a region within the deleted domain that plays an important role in pH-dependent gating. The domain contains a structural element that functionally interacts with the pH sensor in the cytoplasmic $NH_2$-terminus to set a physiological range of pH sensitivity. Removal of the domain shifts the $pK_a$ towards alkaline pH values, causing channel inactivation under physiological conditions. Suppressor mutations within the pH sensor rescued channel gating and trans addition of the cognate peptide restored pH sensitivity. A specific interdomain interaction was revealed in an *in vitro* protein–protein binding assay between the $NH_2$- and COOH-terminal cytoplasmic domains expressed as bacterial fusion proteins. These results provide new insights into the molecular mechanisms underlying Kir channel regulation and channel gating defects that are associated with Bartter's disease.

A definitive link between the Kir1.1 (ROMK or KCNJ1) gene product (Ho *et al.* 1993), the renal secretory $K^+$ channel, and kidney function (Simon *et al.* 1996*b;* Karaloyi & International Collaborative Study Group for Bartter-like Syndromes, 1997) has been established by a familial salt wasting nephropathy called Bartter's syndrome (Bartter *et al.* 1962). Reflecting genetic defects in the renal concentrating mechanism, the disorder is characterized by a constellation of fluid and electrolyte abnormalities, including polyuria, hypokalaemia, metabolic alkalosis and a tendency to develop hypotension despite elevated aldosterone levels (Guay-Woodford, 1998). In fact, loss-of-function mutations in each of the major components of the NaCl reabsorbtive machinery in the thick ascending limb of Henle's loop (TAL) have been linked with this genetically heterogenous disorder (Simon *et al.* 1996*a, b*, 1997; Karaloyi & International Collaborative Study Group for Bartter-like Syndromes, 1997). Consistent with an essential role of the secretory $K^+$ channel in the TAL (Giebisch, 1998), loss-of-function mutations in the *KCN1* (*Kir1.1*) gene co-segregate with Bartter's syndrome.

The discovery of disease-causing mutations in *Kir1.1* not only provides valuable insights into the role of this channel in health and disease, but also lends important clues about structural determinants of function. Like other inward rectifiers, Kir1.1 channels are formed by the tetrameric arrangement of identical subunits. The core domain of each subunit consists of two transmembrane domains and a 'P' loop that contribute to the permeation pathway and the potassium selectivity filter (Nichols & Lopatin, 1997). The cytoplasmic $NH_2$- and COOH-termini, flanking the core domain, contain determinants of channel regulation (Xu *et al.* 1996; Choe *et al.* 1997; MacGregor *et al.* 1998; Huang *et al.* 1998), conduction (Lopatin *et al.* 1994; Wible *et al.* 1994; Yang *et al.* 1995) and oligomerization (Tinker *et al.* 1996; Koster *et al.* 1998). Mutations within each of these domains have pointed to residues that regulate channel permeation and gating (Derst *et al.* 1997, 1998; Karaloyi & International Collaborative Study Group for Bartter-like Syndromes, 1997; Schulte *et al.* 1999). Interestingly, many of the mis-sense mutations appear to cluster around residues that are known to be required for regulation by intracellular pH and PKA (Schulte *et al.*1999).

---

* These authors contributed equally to this work.

Like the native channel (Wang *et al.* 1990), Kir1.1 channels are gated by intracellular pH, closing with cytoplasmic acidification (Tsai *et al.* 1995, Choe *et al.* 1997; McNicholas *et al.* 1998). Recent studies have begun to illuminate the pH-sensing mechanism, whereby two arginine residues in the cytoplasmic $NH_2$- and COOH-termini, R41 and R311, (Fakler *et al.* 1996; Schulte *et al.* 1999) functionally interact with the pH sensor, K80, in the cytoplasmic $NH_2$-terminus (Fakler *et al.* 1996; Schulte *et al.* 1999) to adjust the titration of the residue into a physiological range of pH sensitivity. Underscoring the critical role of pH-dependent gating in physiological regulation of channel activity, recent studies of Leipziger *et al.* (2001) indicate that PKA activation of Kir1.1, involving phosphorylation of residues near the R41–K80–R311 triad (Xu *et al.* 1996), is facilitated by an acid shift in the $pK_a$. Interestingly, Bartter's disease-causing mutations in *Kir1.1* that cluster around the triad, particularly C49Y, I51T, D74Y and L220F, shift the $pK_a$ into the alkaline range and cause channel closure at physiological $pH_i$ (Schulte *et al.* 1999).

We previously reported that a Bartter's disease-causing mutation in *Kir1.1a* (T332 frameshift) that removes a more distal structure – the extreme COOH-terminal 60 amino acids – disrupts channel function by locking the channel in a long-lived closed state (Flagg *et al.* 1999). Here we show that the extreme COOH-terminus acts as an important determinate of Kir1.1 channel gating by intracellular pH. The COOH-terminus contains a structure that appears to be required for an interdomain interaction with the cytoplasmic $NH_2$-terminus, which in turn determines the physiological range of pH sensitivity. Deletion of the domain shifts the open probability–$pH_i$ relation in an alkaline direction, causing channel closure at normal $pH_i$. These results provide new insights into the structural determinants of $pH_i$ gating in the Kir1.1 channel.

## METHODS

### cDNAs and mutagenesis

Mutagenesis was performed by overlap extension PCR (Ho *et al.* 1989). Deletion mutants (Kir1.1a 351X, Kir1.1a 361X and Kir1.1a 388X) were constructed by introducing three stop codons in frame at the appropriate location, as described previously (Flagg *et al.* 1999). All constructs were cloned between 5′ and 3′ untranslated regions of the *Xenopus β-globin* gene in the modified pSD64 vector to increase expression efficiency (Krieg & Melton, 1984). This vector also contains a poly-adenylate sequence in the 3′UTR (dA23dC30). Appropriate cDNA sequences were verified by dye termination sequencing (Applied Biosystem, Foster City, CA, USA).

### cRNA synthesis

Complementary RNA was transcribed *in vitro* in the presence of capping analogue G(5′)ppp(5′)G using *PstI* or *SmaI* linearized cDNA templates. SP6 RNA polymerase was used in all reactions (mMESSAGE mMACHINE; Ambion, Austin, TX, USA). Following DNaseI treatment, cRNA was purified by phenol–chloroform extraction and ammonium acetate/isopropanol precipitation. Yield and concentration were measured spectrophotometrically and confirmed by agarose gel electrophoresis.

### Oocyte isolation and injection

Female *Xenopus laevis* frogs were obtained from NASCO (Fort Atkinson, WI, USA). Standard protocols were followed for the isolation and care of *Xenopus laevis* oocytes. Briefly, frogs were anaesthetized by immersion in 0.15 % 3-aminobenzoate and a partial oophorectomy was performed through an abdominal incision. Oocyte aggregates were manually dissected from the ovarian lobes and then incubated in a calcium-free ORII medium (mM): 82.5 NaCl, 2 KCl, 1 $MgCl_2$, 5 *N*-2-hydroxyethylpiperazine-*N*′-2-ethanesulphonic acid (Hepes)) containing collagenase (Sigma type IA, 2 mg ml$^{-1}$) for ~2 h at room temperature to remove the follicular layer. After oocytes were washed extensively with collagenase-free ORII, they were placed in a modified L15 medium (50 % Leibovitz's medium, 10 mM Hepes, pH 7.4) and stored at 19 °C. Twelve to 24 h after isolation, healthy looking Dumont stage V–VI oocytes were pneumatically injected (PV820 picopump, World Precision Instruments) with 50 nl of water containing 0–50 ng of cRNA and then stored in L15 medium at 19 °C. Channel activity was assessed 1–5 days post-injection. After the final oocyte collection, frogs were humanely killed under anaesthesia. Treatment of frogs followed procedures approved by the Institutional Animal care and use Committee.

### Peptide synthesis and injection

A peptide corresponding to amino acids 332–362 of Kir1.1a (TKEGKYRVDFHNFGKTVEVETPHCAMCLYNE) was synthesized by the Biopolymer Laboratory at the University of Maryland School of Medicine. To increase peptide stability, both ends were capped with an amino group. The lyophilized peptide was resuspended in deionized water and the stock solution (1 mg ml$^{-1}$) stored at −20 °C.

The effects of both acute (injected < 2 h prior to experiment) and chronic (injected 12–24 h prior to experiment) application of the synthetic peptide were examined. In all cases, 50 ng of the peptide was injected. This quantity represents a several order of magnitude molar excess of the peptide compared with the channel based on estimates of channel number from total macroscopic current. Since both acute and chronic peptide application produced the same effect, the data were combined for analysis.

### Recording solutions

The present study is focused on the pH-dependent gating of wild type and mutant forms of Kir1.1a. For the reliable control of intracellular pH in *Xenopus* oocytes, extracellular pH was changed in the presence of a permeant weak acid, butyric acid, as described by Leipziger *et al.* (2001). After incubation in the control 45 mM $K^+$ solution (mM): 45 KCl, 45 *N*-methyl-D-glucamine (NMDG)-Cl, 1 $CaCl_2$, 1 $MgCl_2$ and 5 Hepes, pH 7.4), oocytes were exposed to a modified 45 mM $K^+$ solution containing 3 mM sodium butyrate. Decreasing the pH (7.4, 6.9, 6.4 and 5.4) of the bathing solution (containing butyrate) caused a concomitant decrease in the intracellular pH as assessed with pH-sensitive microelectrodes. Where required, barium acetate was added at a concentration of 1 mM.

### pH microelectrodes and measurement of intracellular pH

Ion-selective microelectrodes were used to monitor intracellular pH ($pH_i$) of oocytes, as previously described (Sciortino & Romero, 1999; Romero *et al.* 1997, 2001). Intracellular ion activity is measured as the difference between the pH electrode and a KCl voltage electrode impaled into the oocyte; and membrane

potential is the potential difference between the KCl micro-electrode and an extracellular calomel electrode (Romero *et al.* 1997). Briefly, pH microelectrodes were fabricated using filamented borosilicate glass pulled to 0.5 $\mu$m tips, silanized at 210 °C with bis-(dimethylamino)-dimethylsilane (Fluka Chemical, Ronkonkoma, NY, USA) and shanks coated with Sylgard (Dow Corning, Midland, MI, USA). Micropipettes were cooled under vacuum, and the tips filled with a $H^+$ ionophore I-cocktail B ion-selective resin (Fluka Chemical, Ronkonkoma, NY) and back-filled with (mM): 40 $KH_2PO_4$, 23 NaOH, 15 NaCl, pH 7.0. The pH electrodes were calibrated using pH 6.0 and 8.0 (traceable National Bureau Standards, Fisher Scientific, Pittsburgh, PA, USA) followed by point calibration. These pH microelectrodes had slopes of at least $-56$ mV (decade change)$^{-1}$.

### Electrophysiology

Whole cell oocyte currents were monitored using a two-micro-electrode voltage clamp equipped with a bath-clamp circuit (OC-725B; Warner, New Haven, CT, USA), as described before (Welling, 1997). Voltage-sensing and current-injecting electrodes had resistances of 0.5–1.5 M$\Omega$ when back-filled with 3 M KCl. After a stable impalement was attained, such that both electrodes measured the same membrane potential, pulse protocols were conducted. Stimulation and data acquisition were performed with a Macintosh Centris 650 computer using an Instrutech ITC16 analog-to-digital, digital-to-analog converter and Pulse software (HEKA, Southboro, MA, USA). Data were filtered at 1 kHz and digitized on-line at 2 kHz to the hard disk using Pulse and IGOR (Wave Metrics, Inc., Lake Oswego, OR, USA) for later analysis.

For macroscopic titration experiments, oocytes were sequentially perfused with a series of gradually decreasing pH solutions. Following stable impalement and assessment of baseline current at $V_m = -100$ mV (500 ms pulse from $V_{hold} = -20$ mV) in the control solution (no butyrate), butyrate-containing solutions at different pH were perfused in succession. Both inward ($V_m = -100$ mV) and outward ($V_m = +40$ mV) currents were monitored every 5 s throughout each experiment ($V_{hold} = -20$ mV). After perfusion of each solution, the current was allowed to reach a new steady state (~5 min after solution exchange) and then measured.

Single-channel properties were assessed 1–5 days post-injection with the patch-clamp technique (Hamill *et al.* 1981). In these studies, the vitelline membrane was removed from oocytes following hyperosmotic shrinking (Methfessel *et al.* 1986). Patch-clamp electrodes, pulled from Corning-Kovar 7052 borsilicate glass, had resistances of 1–5 M$\Omega$. Single-channel currents were measured with an Axopatch 200A patch-clamp amplifier, digitized at a sampling rate of 47 kHz using a VR-10B digital data recorder (Instrutech, Great Neck, NY, 11021) and stored on videotape. Data were acquired and analysed using the Acquire and TAC family of programs (Bruxton Corporation, Seattle, WA USA). Data were replayed, filtered with an eight-pole Bessel filter (Frequency Devices 900) at a cut-off frequency of 1 kHz, and sampled at least five times the filtering frequency. A 50% threshold criterion was used to detect events. Channel open probability, $P_o$, was calculated from 1–3 min continuous records using the equation:

$$P_o = \Sigma(t_1 + t_2 + \dots t_n)/N,$$

where $t_n$ is the fraction open time spent at each of the observed levels and $N$ is the number of levels. In all experiments with mutant channels, data analysis was limited to patches that contained one channel. All analysis of the wild-type channel was limited to patches that contained fewer than or equal to five

channels, as determined by counting the maximum number of current levels during the course of the experiment and/or by determining the final current amplitude following patch excision and channel rundown at the end of an experiment. For $P_o$ diary plots, continuous records were broken into sequential 5–10 s segments, and single-channel open probability was assessed as above. Open and closed dwell-time histograms (logarithmic time scale, 10 bins decade$^{-1}$) were constructed from 15–60 s records containing one channel and fitted to exponential distributions using the Maximum Likelihood Method (Sigworth & Sine, 1987). The single-channel current magnitude was estimated by fitting Gaussian distributions to the current amplitude histograms or by measuring the amplitudes directly from analogue current traces. Inward slope conductance was assessed from such current measurements at $-120$ to $-40$ mV.

### Data analysis

To determine pH-sensitivity, relative current values, $I/I_{max}$, were plotted as a function of pH for each titration experiment and fitted with the modified Hill equation:

$$I/I_{max} = 1/(1 + ([H^+]/K_a)^{n_H}),$$

where $K_a$ is the half-maximal inhibitory proton concentration and $n_H$ is the Hill coefficient. pH sensitivity is reported as the apparent $pK_a$, where $pK_a = -\log(K_a)$. All fits were performed using the IGOR analysis program (Wave Metrics, Inc.) using a non-linear, least squares, iterative algorithm (Levenberg-Marquardt). For the assessment of statistical differences in pH sensitivity, the two numerical determinants of the Hill equation, $K_a$ and $n$, were compared for each of the channels tested. Statistical evaluation of all data was performed with the GB-Stat v5.0.6 for Macintosh statistics package (Dynamic Microsystems, Inc., Silver Spring, MD, USA). Student's *t* test was used for two-group comparisons. ANOVA followed by a Bonferroni test were used for larger group comparisons. The *P* values are listed in the text and figure legends. All data are presented as means ± S.E.M.

### Fusion protein constructs of Kir1.1a

To test for a direct interaction between the cytoplasmic domains of Kir1.1a, recombinant Kir1.1a $NH_2$- and COOH-terminal domains were produced in bacteria as fusion proteins of either glutathione S-transferase (GST) or the maltose binding protein (MBP). A PCR product encoding the cytoplasmic $NH_2$-terminus of Kir1.1 (amino acids 1–60 of Kir1.1b) was cloned in frame with GST in the fusion expression vector, pGEX-5x-3 (Amersham Pharmacia Biotech, Piscutaway, NJ, USA). The GST–Kir1.1 N protein or a GST fusion of the *Shaker* B $NH_2$-terminus (Li *et al.* 1992) was produced in *E. coli* (BL21-RIL codon plus strain, Stratagene, La Jolla, CA, USA), and purified under non-denaturing conditions using glutathione-sepharose 4B affinity chromatography, as recommended by the manufacturer. A PCR product corresponding to the entire cytoplasmic COOH-terminal domain of Kir1.1a, encoding amino acids 183–391, was subcloned in frame with MBP in the MBP-fusion expression vector, pMal-C2 (New England Biolabs, Beverly, MA, USA). The MBP–Kir1.1a C protein was produced in *E. coli* (Top 10 cells, Invitrogen, Carlsbad, CA, USA) and then purified under non-denaturing conditions using amylose resin affinity chromatography, as recommended by the manufacturer.

### Overlay assay

Interaction between the two cytoplasmic domains of Kir1.1 was determined *in vitro* by performing an overlay assay following the methods of Wyszynski & Sheng (1999), as have been employed to elucidate the oligomerization domains in *Shaker* potassium

channels (Li *et al.* 1992) and interdomain interactions in Kir6.2 (Tucker & Ashcroft, 1999; Jones *et al.* 2001) and Kir2.3 channels (Qu *et al.* 2000). Briefly, GST fusion proteins (~0.2 nmol) were resolved by SDS-PAGE (10 % SDS acrylamide) and electrophoretically transferred onto a nitrocellulose membrane (Hybond-ECL, Amersham Pharmacia Biotech). Proteins immobilized on the filter were renatured in gradually decreasing concentrations of guanidine HCl (from 6 M to zero), and then overlaid with MBP–Kir1.1a–C (0.3 $\mu$M) and extensively washed, as described by Wyszynski & Sheng (1999). Blots were probed with Anti-MBP at 1:10 000 (NEB Biolabs) followed by donkey anti-rabbit IgG conjugated to horseradish peroxidase at 1:10 000 (Amersham). An enhanced chemiluminescence system (Amersham) was used to detect bound MBP–Kir1.1a–C according to the manufacturer's instructions.

## RESULTS

We recently reported that truncation of the carboxyl-terminal 60 amino acids of Kir1.1 (Kir1.1 331X) causes a complete loss of channel function (Flagg *et al.* 1999), as
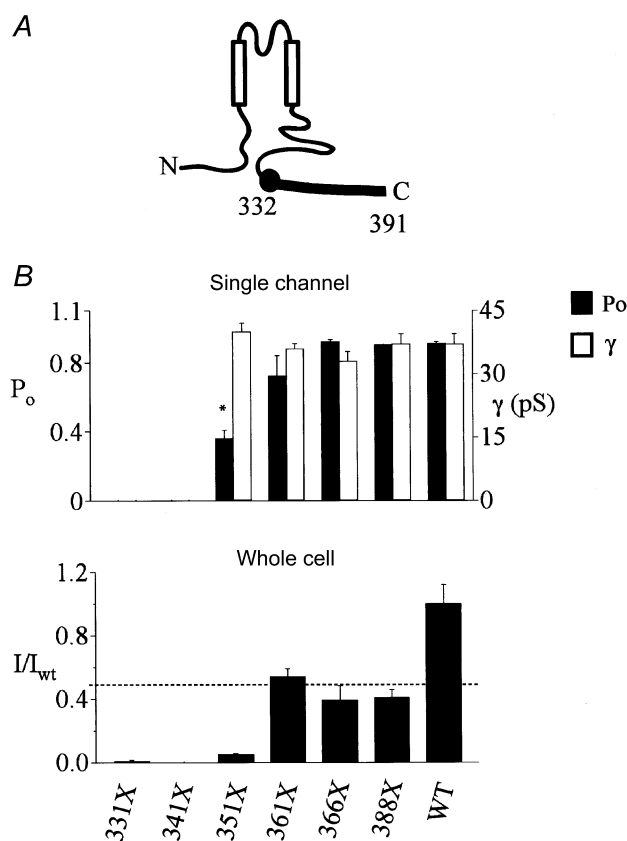


**Figure 1. Channel properties of Kir1.1 COOH-terminal truncation mutants**

*A*, cartoon of Kir1.1 highlighting the cytoplasmic COOH-terminal domain of interest. A series of progressively shorter deletion mutants, from the Bartter's truncation (331X) to the PDZ binding site (388X), were studied. Amino acid 391 is the last amino acid in Kir1.1, *B*). The upper panel summarizes the single-channel open probability ($P_o$) and single-channel conductance ($\gamma$) of the mutants. The lower panel summarizes the whole-cell potassium currents of the mutants relative to wild-type at $-100$ mV (*$P < 0.01$).

would be predicted by the link to Bartter's syndrome. 331X channels reside in an aberrant closed gating conformation (Flagg *et al.* 1999). In order to define the structural basis for the defect, we extended our earlier analysis of mutant channels bearing shorter COOH-terminal truncations, spanning amino acid 331 to the end in roughly 10-residue increments (Fig. 1).

As characterized in *Xenopus* oocytes at the single-channel level by patch-clamp analysis, extension of Kir1.1 331X by 20 amino (351X) was sufficient to rescue minimal channel function, as we reported previously (Flagg *et al.* 1999), and addition of 10 more residues increased open channel probability to a level that is indistinguishable from the wild-type channel. These data define amino acids 332–361 as a structural element that is essential for wild-type channel gating. At the whole cell level, as measured with the two-microelectrode voltage clamp, minimal activity was detected in the 351X channel and macroscopic currents increased further with 361X, qualitatively consistent with what was observed at the single-channel level. However, there was a quantitative discordance between the open probability and the whole cell activity. None of the truncation mutants ever acquired the same level of whole cell activity as the wild-type channel. In fact, removing as little as the last three amino acids (388X), forming a type 1 PDZ binding motif (Fanning & Anderson, 1996), reduced whole cell currents to about one-half those of the wild-type channel. As the single-channel conductance and open probability of 361X, 366X and 388X are identical to the wild-type channel, the decrease in macroscopic activity reflects a significant reduction in the number of *active* channels at the plasma membrane.

Collectively, these studies reveal two distinct structural determinants of channel function. The distal domain, requiring at least the last three amino acids, is required for maintaining the number of active channels at the plasma membrane, possibly reflecting the presence of an endoplasmic reticulum (ER) export signal (Ma *et al.* 2001) and PDZ-based trafficking and retention signals (Fanning & Anderson, 1996). In contrast, the proximal domain (332–361) appears to be an important determinant of channel gating behaviour. In the remainder of the study, we focus on elucidating the molecular mechanism for altered gating by studying the basis for the defect in the minimally active 351X channel.

The altered gating behaviour of the Kir1.1a 351X channel that we previously reported was confirmed in single-channel, cell-attached patch-clamp recordings (Fig 2). In contrast to the sustained high open probability kinetics of the wild-type channel, the Kir1.1a 351X mutant exhibited bursts of channel activity interrupted by sojourns in a closed gating mode. In some cases, the 351X channel permanently entered a closed state. As a consequence, the time-averaged (3 min) open probability of the channel
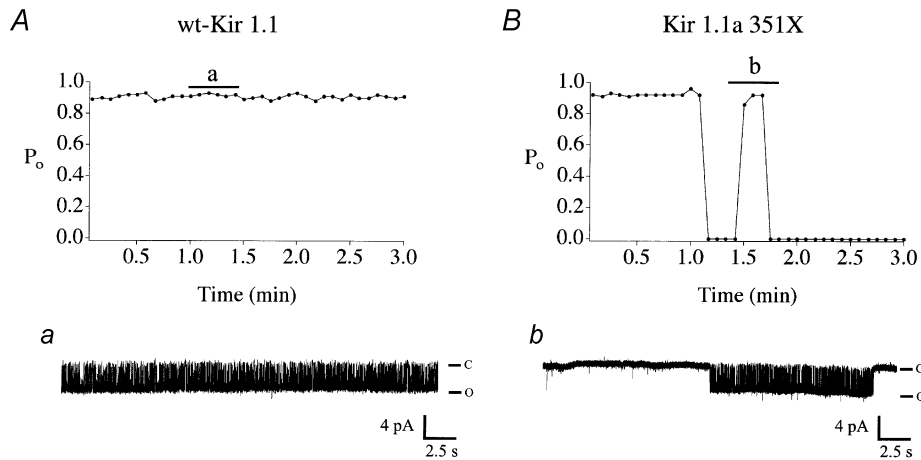
**Figure 2. COOH-terminal truncation induces an aberrant gating mode**

Diary plots of single-channel open probability, $P_o$ of wild-type Kir1.1a (*A*) *vs.* the truncated mutant, Kir1.1a 351X (*B*). Shown are plots of $P_o$ measured in 5 s intervals over the duration of a 3 min recording. Representative channel records corresponding to the indicated time are shown in *a* and *b*. Single-channel recordings were obtained in the cell-attached mode ($V_m = -80$ mV) from oocytes injected with either wild-type or mutant channel cRNA.

was reduced ($0.55 \pm 0.14$, $n = 6$) compared with the wild-type channel ($0.90 \pm 0.01$, $n = 6$).

### Kir1.1a 351X is more sensitive to intracellular pH than the wild-type channel

The altered gating phenotype of the Kir1.1a 351X channel is reminiscent of the wild-type channel undergoing pH-dependent channel closure. To determine whether the COOH-terminal domain might be playing a role in pH-dependent gating, we compared the $pH_i$ sensitivity of the 351X channel to the wild-type Kir1.1a.

Channel activity was determined in intact cells to safeguard against any possibility of excision-induced channel rundown phenomena (McNicholas *et al.* 1994; Huang *et al.* 1998). Because Kir1.1 is insensitive to extra-cellular pH (Tsai *et al.* 1995), $pH_i$-dependent changes in channel activity can be accurately determined in intact oocytes by changing extracellular pH in the presence of a permeant weak acid like butyrate (Leipziger *et al.* 2001). Intracellular pH measurements were performed to construct a titration curve. A representative experiment is shown in Fig 3*A*. There were no significant differences between $pH_i$ measured in oocytes expressing either the mutant or the wild-type channel. Consequently, average $pH_i$ data were pooled to construct a $pH_i$–$pH_o$ curve for all subsequent titration experiments (Fig 3*B*).

Macroscopic currents were measured at the different internal pH values using two-microelectrode voltage clamp. As shown in Fig 4, Kir1.1a 351X was markedly more sensitive to intracellular acidification than the wild-type channel. The 351X mutation shifted the apparent $pK_a$ from $6.63 \pm 0.04$ ($n = 16$) to $7.00 \pm 0.04$ (wild-type, $n = 15$) without significantly changing the highly co-operative process ($h = 5.15 \pm 0.73$, 351X, and $6.90 \pm 2.25$, wild-type).

The result was confirmed at the single-channel level. In these studies, open probability was monitored in cell-attached patches at resting intracellular pH ($\sim$7.2) in control solution and then at an intracellular pH of 6.68
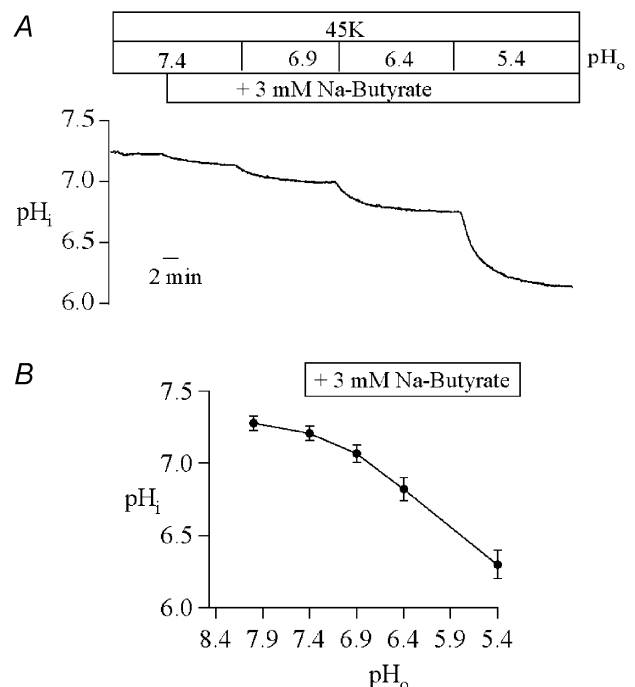


**Figure 3. Intracellular pH in oocytes as a function of extracellular pH and butyrate**

*A*, typical titration in a *Xenopus* oocyte injected with wild-type Kir1.1a cRNA. Identical results were obtained for oocytes injected with Kir1.1a 351X cRNA. Butyrate was added and the pH of the 45 mM $K^+$ bathing solution was changed as indicated. Intracellular pH was measured with intracellular pH-sensitive microelectrodes every 2 s for the duration of the record. *B*, the mean steady-state $pH_i$ in each of the bathing solutions is summarized.

in the 3 mM sodium butyrate, pH 6.4 solution. Typical results are shown in Fig. 5. As predicted by the macroscopic titration curves, the Kir1.1a 351X open probability was significantly reduced in the pH 6.4 solution ($\Delta P_o = -0.41 \pm 0.14$, $n = 3$), while the open probability of the wild-type channel remained nearly unchanged ($\Delta P_o = -0.14 \pm 0.12$, $n = 3$).

These data demonstrate that the extreme COOH-terminus plays an important role in determining pH-dependent gating. Removal of the domain shifts the apparent p$K_a$ in an alkaline direction, as would be predicted if the COOH-

terminus normally participates in shielding the pH sensor from proton attack. In this case, the altered gating kinetics of the Kir1.1a 351X channel reflects the increased probability of K80 protonation and thus inactivation at physiological pH$_i$. The hypothesis predicts that rendering the Kir1.1a 351X channel insensitive to pH$_i$ should rescue normal channel function.

## A suppressor mutation within the pH sensor (K80M) restores channel function

Replacement of K80 with the corresponding non-titratable methionine residue of Kir2.1, a pH-insensitive inward rectifying K$^+$ channel, completely abolished pH-dependent gating of Kir1.1 (Fakler *et al.* 1996). The reverse mutation, M84K in Kir2.1, introduced dependence on pH$_i$ similar to the wild-type Kir1.1a channel (Fakler *et al.* 1996). Accordingly, we introduced a K80M mutation in Kir1.1a 351X channels (Kir1.1a 351X/K80M) to suppress the pH sensor and remove the pH-dependent gating process.
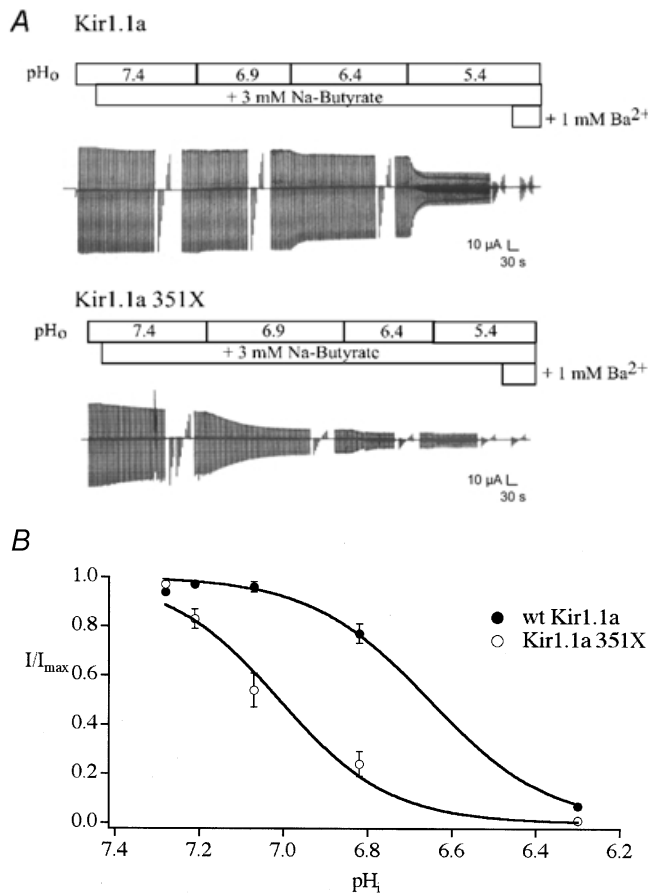


**Figure 4. Kir1.1a 351X channels are more sensitive to gating by cytoplasmic pH than wild-type channels**

*A*, titration of macroscopic channel activity in oocytes injected with either Kir1.1a (250 pg) or Kir1.1a 351X (2.5 ng) cRNA. Representative experiments are shown. The modified 45 mM K$^+$ solutions containing butyrate, at different pH values, were perfused as indicated, and current was monitored throughout the course of the solution change ($V_{hold} = -20$ mV, $\sim E_K$, stepped to $-100$ and $+40$ mV every 5 s). Continuous current record was occasionally interrupted for current–voltage assessment ($-100$ to $-40$ mV in 20 mV steps). *B*, steady-state macroscopic currents ($I/I_{max}$, $V_m = -100$ mV) were plotted as a function of pH$_i$ for each titration experiment ($n = 15$–$16$) and fitted with the modified Hill equation: $I/I_{max} = 1 / 1 + ([H^+]/K_a^{n_H})$, where $K_a$ is the proton concentration at half-maximal inhibition and $n_H$ is the Hill coefficient. Kir1.1a 351X channels are significantly more sensitive to pH$_i$ (p$K_a = 7.00 \pm 0.04$) than wild-type Kir1.1a (p$K_a = 6.63 \pm 0.04$).
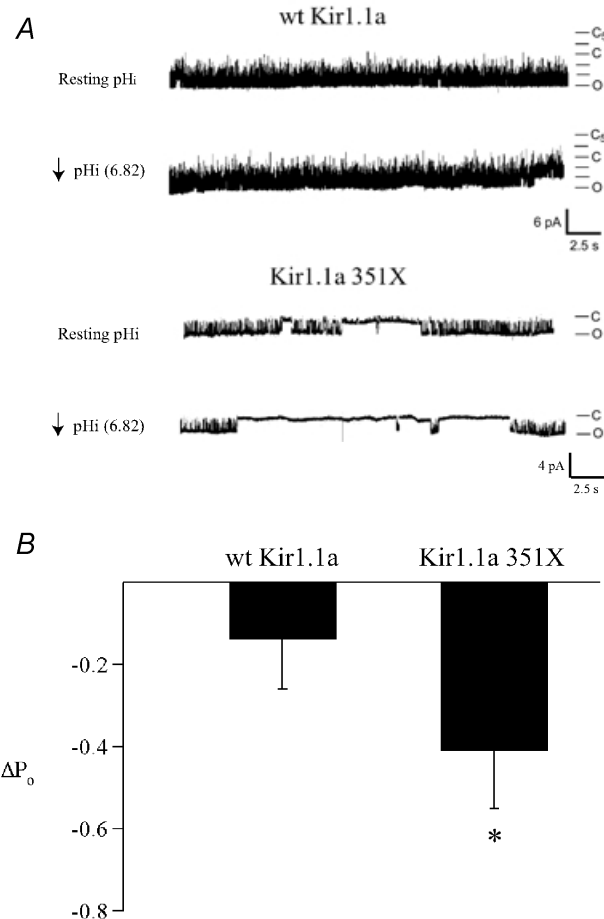


**Figure 5. Increased pH sensitivity of Kir1.1a 351X at the single-channel level**

*A*, representative cell-attached patch recordings at resting pH$_i$ (7.28) and upon intracellular acidification (pH$_i = 6.82$; $V_m = -80$ mV) from oocytes expressing either wild-type or mutant channels. *B*, summarized data showing the change in open probability upon intracellular acidification for wild-type and mutant channel (351X; *$P < 0.01$).

We first compared the macroscopic current density in *Xenopus* oocytes injected with either Kir1.1a 351X, Kir1.1a 351X/K80M or wild-type Kir1.1a cRNA. As predicted by our hypothesis, substitution of methionine for lysine 80 removed channel pH sensitivity (data not shown) and rescued Kir1.1a 351X function (Fig. 6). The $Ba^{2+}$-sensitive inward current measured in oocytes expressing Kir1.1a 351X/K80M was significantly increased ($I = -13.09 \pm 1.93$ $\mu A$, $n = 9$) compared with Kir1.1a 351X ($I = -1.09 \pm 0.16$ $\mu A$, $n = 10$) at $V_m = -100$ mV. In fact, the macroscopic current density of the Kir1.1a 351X/K80M increased to about one-half the level of the wild-type channel, as would be predicted if the suppressor mutation, K80M, specifically rescued a gating defect involving the proximal domain. The increase in channel activity was specific for Kir1.1a 351X; replacement of lysine 80 with methionine had no effect on wild-type current density because the wild-type channel is normally active at physiological pH. The observation was confirmed at the single-channel level in long duration cell-attached patch recordings (3 min). In contrast to the lower average $P_o$ of Kir1.1a 351X ($0.55 \pm 0.10$, $n = 6$), Kir1.1a 351X/K80M

exhibit an average $P_o$ ($0.89 \pm 0.01$, $n = 6$) which is identical to the wild-type channel ($0.90 \pm 0.01$, $n = 6$). Moreover, the mean open time ($16.32 \pm 1.09$ *vs.* $15.98 \pm 1.03$ ms), mean closed time ($1.05 \pm 0.08$ *vs.* $1.28 \pm 0.06$ ms) and single-channel conductance ($37.5 \pm 2$ *vs.* $36.9 \pm 5$ pS) did not differ between the K80M/351X and the wild-type channel, respectively.

## Interdomain interactions between cytoplasmic $NH_2$- and COOH-termini

Our model predicts that the intracellular $NH_2$-terminal and COOH-terminal domains of Kir1.1 should physically interact with one another. To test this hypothesis, we developed an *in vitro* protein–protein interaction assay between the two cytoplasmic domains of Kir1.1 expressed as fusion proteins in bacteria. Recombinant $NH_2$-terminal and COOH-terminal domains were made as glutathione S-transferase (GST) and maltose-binding protein (MBP) fusions, respectively, in *E. coli* and then purified to homogeneity under non-denaturing conditions using glutathione-sepharose 4B or amylose resin affinity chromatography (see Fig. 7*A* and *B*). The GST protein alone, the $NH_2$-terminal Kir1.1–GST fusion protein or
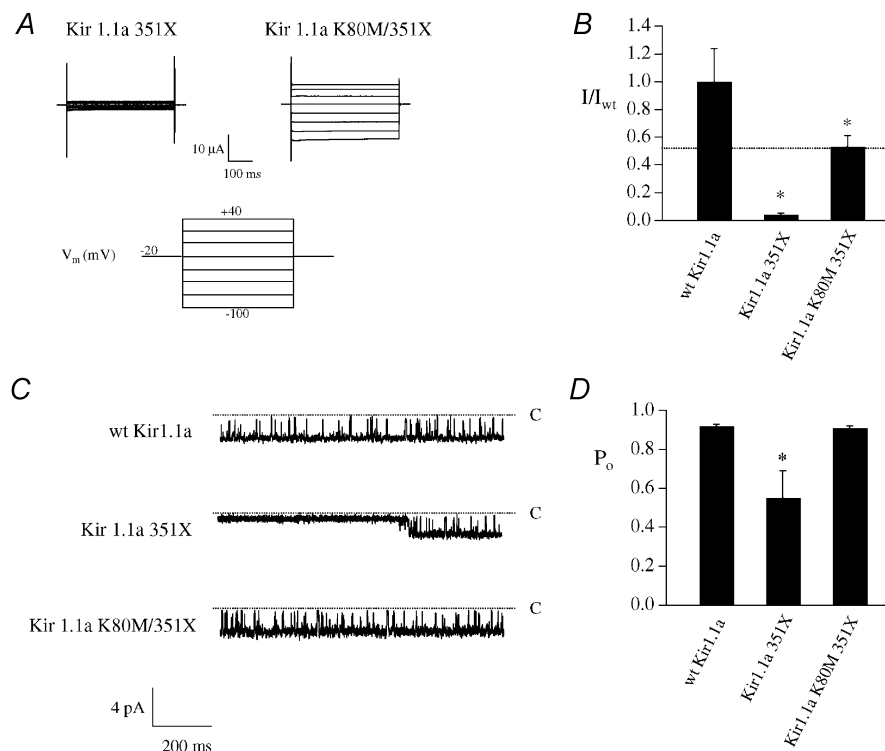


**Figure 6. A suppressor mutation in the pH sensor (K80M) rescues Kir1.1a 351X function, restoring high open probability gating kinetics**

*A*, representative families of whole-cell currents measured in *Xenopus* oocytes injected with either Kir1.1a 351X or Kir1.1a 351X/K80M cRNA (250 pg). Currents were obtained using two-microelectrode voltage clamp (45 mM $K_o^+$, $V_{hold} = -20$ mV, stepped in 20 mV increments from $-100$ to $+40$ mV). *B*, summarized data of whole-cell potassium current relative to wild-type at $-100$ mV. *C*, single-channel records obtained in symmetrical 150 mM KCl from oocytes injected with either wild-type or mutant cRNA in the cell-attached configuration ($V_m = -80$ mV). Inward currents are shown and upward deflections represent channel closures. *D*, average open probabilities ($P_o$) for both wild-type and mutant channels over the duration of 3 min traces (*$P < 0.01$).

GST fusion of the $NH_2$-terminal domain of the *Shaker* B channel (Li *et al.* 1992) were resolved by SDS-PAGE, immobilized on nitrocellulose, renatured and then probed with the MBP–Kir1.1 COOH-terminal fusion protein. The results of a typical overlay are shown in Fig. 7*C*. The GST protein alone or a GST fusion of the $NH_2$-terminal domain of the *Shaker* B channel did not interact with the MBP fusion. In contrast, the MBP–Kir1.1 COOH-terminal fusion protein strongly bound to the GST $NH_2$-terminal domain of Kir1.1. Specific interaction between the GST $NH_2$-terminus and the MBP–Kir1.1 COOH-terminus was observed over a wide pH range (5.7–7.4). No interaction was observed with the MBP fusion alone. Collectively, the study provides strong evidence that the $NH_2$- and COOH-terminal domains of Kir1.1 specifically associate with one another.

## Delimiting amino acids responsible for regulating pH-dependent gating

To demarcate the region within the extreme COOH-terminus of the channel that is responsible for determining pH-dependent gating, pH-sensitivity of a series of truncated channels (351X, 361X and 388X) was assessed and compared with the wild-type channel. As shown in Fig. 8*A*, only Kir1.1a 351X was more susceptible to gating by intracellular protons (apparent $pK_a = 7.00 \pm 0.04$ in 351X compared with $6.63 \pm 0.04$ in wild-type). None of the other mutant channels tested exhibited an apparent $pK_a$ that was significantly different from the wild-type channel ($pK_a = 6.49 \pm 0.04$ in 361X and $6.59 \pm 0.09$ in 388X). These observations define a COOH-terminal domain, encoded by amino acids 332–361, that determines Kir1.1a pH-sensitivity. The region is identical to what we earlier defined (see Fig. 1) as a structural element that is
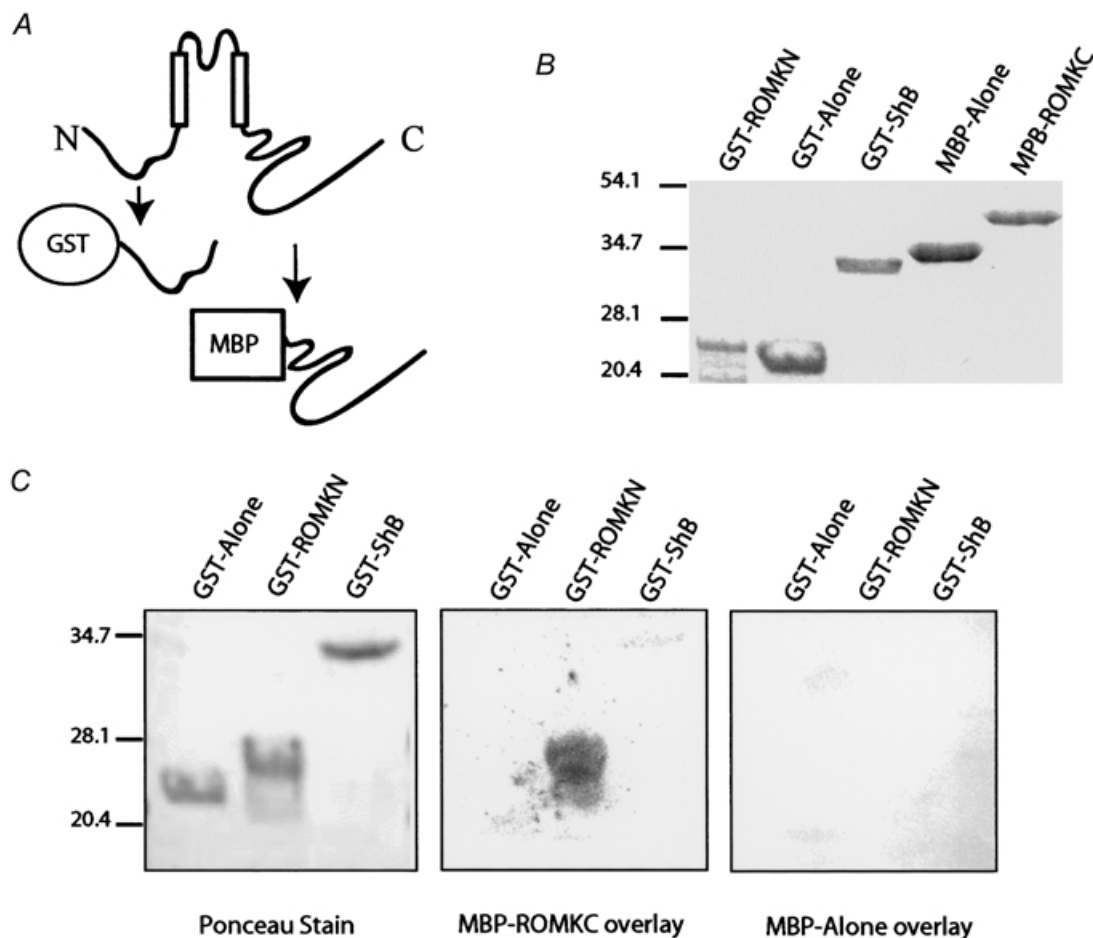


**Figure 7. Cytoplasmic $NH_2$- and COOH-terminal domains of Kir1.1 interact *in vitro***

*A*, cartoon illustrating the cytoplasmic domains of Kir1.1 and the corresponding bacterial fusion proteins. The $NH_2$-domain was made as a GST fusion and the COOH-domain was made as a MBP fusion. *B*, purified recombinant domains resolved by SDS-PAGE and visualized by Coomassie Brillant Blue staining. *C*, gel overlay assay: GST alone or GST fusions of the *Shaker* B cytoplasmic $NH_2$-terminus (GST–ShB) or the Kir1.1 N-terminus (GST–ROMKN) were resolved by SDS-PAGE, transferred to nitrocellulose, renatured, visualized by Ponceau staining (left) and then blotted with either the MBP protein alone (right) or MBP fusion of the Kir1.1 COOH-terminal domain (MBP–ROMKC, middle). After extensive washes, bound MBP protein was detected using an anti-MBP antibody.

essential for appropriate channel gating, effectively linking the two processes.

If the COOH-terminal domain (332–361) determines pH sensitivity by protecting the pH sensor from proton attack, the domain should rescue mutant 351X channel function in trans. Accordingly, we assessed pH sensitivity of 351X and wild-type channels in oocytes injected with a synthetic peptide (50 ng) corresponding to amino acids 332–362 of Kir1.1a. As shown in Fig. 8*C*, the synthetic peptide partially restored the pH sensitivity of Kir1.1a 351X, shifting the apparent $pK_a$ from 7.00 to $6.88 \pm 0.03$ ($n = 15$) towards the wild-type $pK_a$ of 6.63. In contrast, the peptide had no effect on the wild-type channel ($n = 8$); in the presence of the peptide the $pK_a$ of the wild-type channel was $6.56 \pm 0.03$, no different from the wild-type channel without the peptide ($6.63 \pm 0.04$). Interestingly, the peptide did not restore channel function in the completely inactive 331X channel, presumably because these channels enter an irreversible closed state. Nevertheless, the results with the defective 351X channel clearly demonstrate that the COOH-terminal domain functionally interacts with the $NH_2$-terminal pH sensor to shift the $pK_a$ in an acid direction, allowing the channel to stay open at physiological intracellular pH.

## DISCUSSION

A Bartter's disease mutation in the Kir1.1 channel removes the last 60 amino acids (Simon *et al.* 1996*b*) and induces an aberrant 'locked–closed' gating conformation (Flagg *et al.* 1999). In the present study, we have elucidated the molecular mechanism. Our data identify a domain within the COOH-terminus that controls $pH_i$-dependent channel gating. Truncating the domain by disease or artificial mutation produces an alkaline shift in the current–$pH_i$ relation, causing channel inactivation at normal intracellular pH. Because the pH-dependent gating machinery remains intact, the observation indicates that the COOH-terminal domain usually co-ordinates the effective range of the pH sensor. Reinforcing this view, we found that a suppressor mutation within the pH sensor restored wild-type high open probability gating on the 351X truncated channel. Collectively, the data demonstrate that the COOH-terminal domain normally participates in pH-dependent gating, presumably interacting with, or nearby to the pH sensor.

A single lysine, K80, which is found in the cytoplasmic $NH_2$-terminus close to the first transmembrane domain, acts as the pH sensor in the Kir1.1 channel (Fakler *et al.* 1996). Although protonation of the residue triggers



**Figure 8. Residues 332–361 form an intrasteric pH-regulatory domain**

To delimit the COOH-terminal pH-gating determinant, the pH sensitivity of the COOH-terminal truncation mutants were determined. In contrast to Kir1.1a 351X, the pH sensitivities of both Kir1.1a 361X and Kir1.1a 388X were identical to wild-type channel (*A*). These data identify amino acids 332–361 as an essential pH-dependent gating element (*B*). Consistent with an intrasteric regulatory role of this domain, injection of a synthetic peptide corresponding to amino acids 332–362 partially restored the pH sensitivity ($pK_a = 6.88 \pm 0.03$, $n = 15$) of Kir1.1a 351X. The peptide had no effect on wild-type channel ($n = 8$). The $pK_a$ of wild-type channel in the presence of the peptide was $6.56 \pm 0.03$. ●, 351X + peptide; ■, wild-type + peptide superimposed on 351X or wild-type titration curves (dotted lines) (*C*).
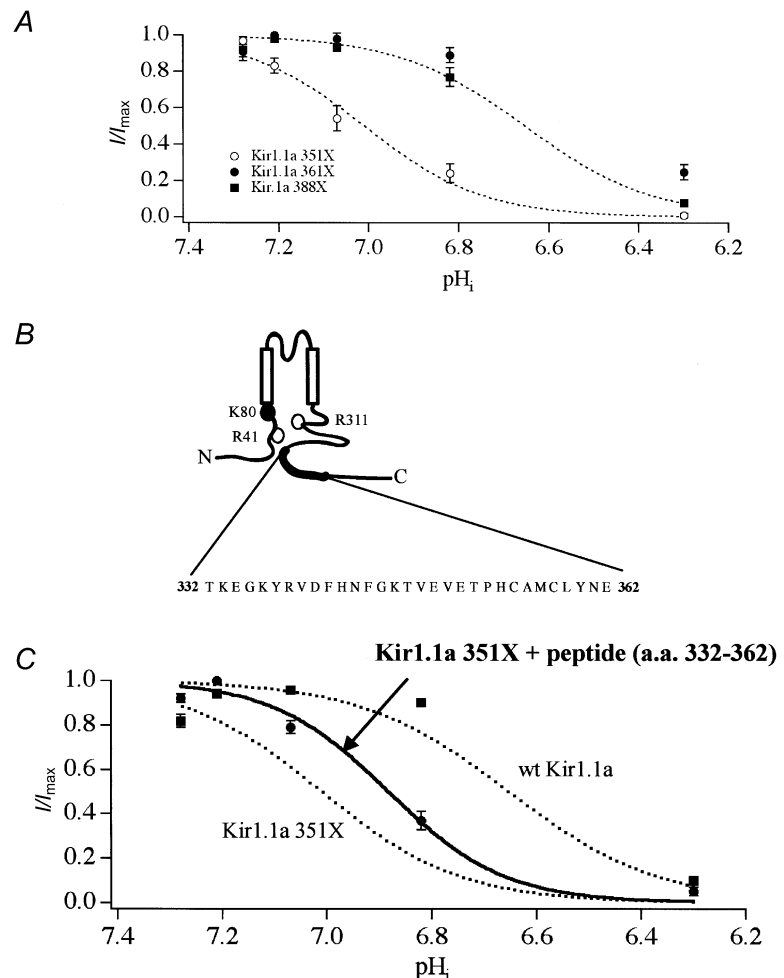
channel closure (Fakler *et al.* 1996; Schulte *et al.* 1999), Kir1.1 are normally open at physiological pH$_i$ because titration of K80 is anomalous, occurring in the neutral pH range, far from the predicted p$K_a$ of a free lysine (p$K_a$~10). The response indicates that other structures in the Kir1.1 protein shield the pH sensor from proton attack. For instance, structural studies in ovotransferrin and human transferrin indicate that interdomain interactions between side chains of two lysines cause a dramatic acid shift in the p$K_a$ of the two titratable residues, important for the pH-sensitive transferrin ion binding and release mechanism (Dewan *et al.* 1993; Fakler *et al.* 1996; He *et al.* 1999). Similar to this model, Schulte *et al.* recently provided compelling evidence for two arginine residues – R41 and R311 – in distant NH$_2$- and COOH-termini that interact in close spatial proximity with the pH sensor to form an electrostatic shield which shifts the p$K_a$ of K80 into the neutral range (Schulte *et al.* 1999).

Our data identify a more distant structure, encoded by amino acids 332–361, that also determines Kir1.1a pH-dependent gating by setting the range of the pH sensor. The cognate synthetic peptide partially restored pH-sensitivity in the 351X channel but had no effect on the wild-type channel, strongly suggesting that the COOH-terminal domain usually forms interdomain contacts close to the pH sensor or with other structures that stabilize electrostatic interactions of R41 and R311. Supporting this model, we found that the COOH-terminus is capable of interacting with the cytoplasmic NH$_2$-terminus *in vitro*. Unlike the pH-dependent interaction between NH$_2$- and COOH-terminal domains reported for Kir2.3 (Qu *et al.* 2000) channel, interaction between the cytoplasmic domains of Kir1.1 was detected over a wide pH range, perhaps more similar to what has been reported for the Kir6.2 channel (Tucker *et al.* 1999). Collectively, the data imply a relatively pH stable tertiary structure of the Kir1.1 channel in which the extreme COOH-terminus folds onto the NH$_2$-terminus to form an electrostatic pocket around the pH sensor near the first transmembrane domain.

It remains to be determined whether the COOH-terminal structure contributes to physiological regulation of channel activity, acting in a matter similar to intrasteric regulatory domains in protein kinases and phosphatases (Kobe & Kemp, 1999), which control catalytic activity by reversibly and directly binding to the active site. Interestingly, the COOH-terminal domain in Kir1.1 exhibits a degree of amino acid conservation, sharing about 30 % identity with other members of the inward rectifying channel family. Structure–function studies in Kir6.2, the pore-forming subunit of $\beta$-islet cells and cardiac K$^+$ channels, indicate that residues within both the NH$_2$- and COOH-termini act to control ATP sensitivity (Tucker *et al.* 1998; Drain *et al.* 1998; Shyng & Nichols, 1998; Koster *et al.* 1999; Enkvetchakul *et al.* 2001). In

particular, Drain *et al.* identified a structural determinant of ATP-dependent gating that lies within this moderately conserved domain (Drain *et al.* 1998). These observations suggest a widespread modulatory function of this structure in Kir channels.

In contrast to the pH sensor, the pH-dependent gating machinery has not been precisely identified. In the two-transmembrane domain potassium channel from *Streptomyces lividans*, KcsA, extracellular acidification induces a large conformational change in the COOH-terminal end of the second transmembrane helix, which presumably reduces the diameter of the internal vestibule of the pore to alter the conduction pathway (Perozo *et al.* 1998). Several studies have offered evidence for a similar mechanism in Kir1.1 channels. For instance, recent work by Schulte *et al.* suggests that pH gating and K$^+$-dependent gating are coupled via structural rearrangements in the inner pore, presumably involving the P-helix (Schulte *et al.* 2001). Moreover, pH-dependent conformational changes in the cytoplasmic NH$_2$- and COOH-termini have been observed by examining state-dependent chemical modification of cysteine residues with sulphydryl reagents (Schulte *et al.* 1998). The only cysteine residues (C49 and C308) that acquire thiol reactivity in a pH state-dependent manner lie in close proximity to the critical arginine residues of the R–K–R triad, raising the intriguing possibility that the gating machinery is directly conjoined with the neighbouring pH sensor. If such a model is accurate, structures modulating the pH sensor, such as the COOH-domain, may also directly control the efficacy of pH-dependent gating.

In summary, we have elucidated the molecular mechanism underlying the loss of channel function by a Bartter's disease mutation. Our data reveal a previously unappreciated structure within the extreme COOH-terminus that normally interacts near the pH sensor in the cytoplasmic NH$_2$-terminus to set a physiological range of pH sensitivity. Deletion of the domain shifts the open probability–pH$_i$ relation in alkaline shift, causing channel inactivation at normal intracellular pH. Our results imply a tertiary structure of Kir1.1 in which the extreme COOH-terminus interacts with the NH$_2$-terminus and raises the possibility that similar interdomain interactions may underscore the regulation and gating of other Kir channels.

## REFERENCES

BARTTER, F. C., PRONOVE, P., GILL, J. R. JR & MACCARDLE, R. C. (1962). Hyperplasia of the juxtaglomerular complex with hyperaldosteronism and hypokalemic alkalosis: a new syndrome. *American Journal of Medicine* **33**, 811–828.

CHANCHEVALAP, S., YANG, Z., CUI, N., QU, Z., ZHU, G., LIU, C., GIWA, L. R., ABDULKADIR, L. & JIANG, C. (2001). Involvement of histidine residues in proton sensing of ROMK1 channel. *Journal of Biological Chemistry* **275**, 7811–7817.

CHOE, H., ZHOU, H., PALMER, L. G. & SACKIN, H. (1997). A conserved cytoplasmic region of ROMK modulates pH sensitivity, conductance, and gating. *American Journal of Physiology* **273**, F516–529.

DERST, C., KONRAD, M., KOCKERLING, A., KAROLYI, L., DESCHENES, G., DAUT, J. & SEYBERTH, H. W. (1997). Mutations in the ROMK gene in antenatal Bartter syndrome are associated with impaired K⁺ channel function. *Biochemical and Biophysical Research Communications* **230**, 641–645.

DERST, C., WISCHMEYER, E., PREISIG-MULLER, R., SPAUSCHUS, A., KONRAD, M., HENSEN, P., JECK, N., SEYBERTH, H. W., DAUT, J. & KARSCHIN, A. (1998). A hyperprostaglandin E syndrome mutation in Kir1.1 (renal outer medullary potassium) channels reveals a crucial residue for channel function in Kir1.3 channels. *Journal of Biological Chemistry* **273**, 23884–23891.

DEWAN, J. C., MIKAMI, B., HIROSE, M. & SACCHETTINI, J. C. (1993). Structural evidence for a pH-sensitive dilysine trigger in the hen ovotransferrin N-lobe: implications for transferrin iron release. *Biochemistry* **32**, 11963–11980.

DRAIN, P., LI, L. & WANG, J. (1998). $K_{ATP}$ channel inhibition by ATP requires distinct functional domains of the cytoplasmic C terminus of the pore-forming subunit. *Proceedings of the National Academy of Sciences of the USA* **95**, 13953–13958.

ENKVETCHAKUL, D., LOUSSOUARN, G., MAKHINA, E., SHYNG, S. L. & NICHOLS, C. G. (2001). The kinetic and physical basis of K(ATP) channel gating: toward a unified molecular understanding. *Biophysical Journal* **78**, 2334–2348.

FAKLER, B., SCHULTZ, J. H., YANG, J., SCHULTE, U., BRANDLE, U., ZENNER, H. P., JANL, Y. & RUPPERSBERG, J. P. (1996). Identification of a titratable lysine residue that determines sensitivity of kidney potassium channels (ROMK) to intracellular pH. *EMBO Journal* **15**, 4093–4099.

FANNING, A. S. & ANDERSON, J. M. (1996). Protein–protein interactions: PDZ domain networks. *Current Biology* **6**, 1385–1388.

FLAGG, T. P., TATE, M., MEROT, J. & WELLING, P. A. (1999). A mutation linked with Bartter's syndrome locks Kir1.1a (ROMK1) channels in a closed state. *Journal of General Physiology* **114**, 685–700.

GIEBISCH, G. (1998). Renal potassium transport: mechanisms and regulation. *American Journal of Physiology* **274**, F817–833.

GUAY-WOODFORD, L. M. (1998). Bartter syndrome: unraveling the pathophysiologic enigma. *American Journal of Medicine* **105**, 151–161.

HAMILL, O. P., MARTY, A., NEHER, E., SAKMANN, B. & SIGWORTH, F. J. (1981). Improved patch-clamp techniques for high-resolution current recording from cells and cell-free membrane patches. *Pflügers Archiv* **391**, 85–100.

HE, Q. Y., MASON, A. B., TAM, B. M., MACGILLIVRAY, R. T. & WOODWORTH, R. C. (1999). Dual role of Lys206–Lys296 interaction in human transferrin N-lobe: iron-release trigger and anion-binding site. *Biochemistry* **38**, 9704–9711.

HO, K., NICHOLS, C. G., LEDERER, W. J., LYTTON, J., VASSILEV, P. M., KANAZIRSKA, M. V. & HEBERT, S. C. (1993). Cloning and expression of an inwardly rectifying ATP-regulated potassium channel. *Nature* **362**, 31–38.

HO, S. N., HUNT, H. D., HORTON, R. M., PULLEN, J. K. & PEASE, L. R. (1989). Site-directed mutagenesis by overlap extension using the polymerase chain reaction. *Gene* **77**, 51–59.

HUANG, C. L., FENG, S. & HILGEMANN, D. W. (1998). Direct activation of inward rectifier potassium channels by PIP2 and its stabilization by $G_{\beta\gamma}$. *Nature* **391**, 803–886.

JONES, P. A., TUCKER, S. J. & ASHCROFT, F. M. (2001). Multiple sites of interaction between the intracellular domains of an inwardly rectifying potassium channel, Kir6.2. *FEBS Letters* **508**, 85–89.

KARALOYI, L. & INTERNATIONAL COLLABORATIVE STUDY GROUP FOR BARTTER-LIKE SYNDROMES (1997). Mutations in the gene encoding the inwardly-rectifying renal potassium channel, ROMK, cause the antenatal variant of Bartter syndrome: evidence for genetic heterogeneity. *Human Molecular Genetics* **6**, 17–26.

KOBE, B. & KEMP, B. E. (1999). Active site-directed protein regulation. *Nature* **402**, 373–36.

KOSTER, J. C., BENTLE, K. A., NICHOLS, C. G. & HO, K. (1998). Assembly of ROMK1 (Kir1.1a) inward rectifier K⁺ channel subunits involves multiple interaction sites. *Biophysical Journal* **74**, 1821–1829.

KOSTER, J. C., SHA, Q., SHYNG, S. & NICHOLS, C. G. (1999). ATP inhibition of $K_{ATP}$ channels: control of nucleotide sensitivity by the N-terminal domain of the Kir6.2 subunit. *Journal of Physiology* **515**, 19–30.

KRIEG, P. A. & MELTON, D. A. (1984). Functional messenger RNAs are produced by SP6 *in vitro* transcription of cloned cDNAs. *Nucleic Acids Research* **12**, 7057–7070.

LEIPZIGER, J., MACGREGOR, G. G., COOPER, G. J., XU, J., HEBERT, S. C. & GIEBISCH, G. (2001). PKA site mutations of ROMK2 channels shift the pH dependence to more alkaline values. *American Journal of Physiology – Renal Physiology* **279**, F919–926.

LI, M., JAN, Y. N. & JAN, L. Y. (1992). Specification of subunit assembly by the hydrophilic amino-terminal domain of the *Shaker* potassium channel. *Science* **257**, 1225–1230.

LOPATIN, A. N., MAKHINA, E. N. & NICHOLS, C. G. (1994). Potassium channel block by cytoplasmic polyamines as the mechanism of intrinsic rectification. *Nature* **372**, 366–369.

MA, D., ZERANGUE, N., LIN, Y. F., COLLINS, A., YU, M., JAN, Y. N. & JAN, L. Y. (2001). Role of ER export signals in controlling surface potassium channel numbers. *Science* **291**, 316–339.

MACGREGOR, G. G., XU, J. Z., MCNICHOLAS, C. M., GIEBISCH, G. & HEBERT, S. C. (1998). Partially active channels produced by PKA site mutation of the cloned renal K⁺ channel, ROMK2 (kir1.2). *American Journal of Physiology* **275**, F415–422.

MCNICHOLAS, C. M., MACGREGOR, G. G., ISLAS, L. D., YANG, Y., HEBERT, S. C. & GIEBISCH, G. (1998). pH-dependent modulation of the cloned renal K⁺ channel, ROMK. *American Journal of Physiology* **275**, F972–981.

MCNICHOLAS, C. M., WANG, W., HO, K., HEBERT, S. C. & GIEBISCH, G. (1994). Regulation of ROMK1 K⁺ channel activity involves phosphorylation processes. *Proceedings of the National Academy of Sciences of the USA* **91**, 8077–8081.

METHFESSEL, C., WITZEMANN, V., TAKAHASHI, T., MISHINA, M., NUMA, S. & SAKMANN, B. (1986). Patch clamp measurements on *Xenopus laevis* oocytes: currents through endogenous channels and implanted acetylcholine receptor and sodium channels. *Pflügers Archiv* **407**, 577–588.

NICHOLS, C. G. & LOPATIN, A. N. (1997). Inward rectifier potassium channels. *Annual Review of Physiology* **59**, 171–191.

PEROZO, E., CORTES, D. M. & CUELLO, L. G. (1998). Three-dimensional architecture and gating mechanism of a K⁺ channel studied by EPR spectroscopy. *Nature Structural Biology* **5**, 459–469.

QU, Z., YANG, Z., CUI, N., ZHU, G., LIU, C., XU, H., CHANCHEVALAP, S., SHEN, W., WU, J., LI, Y. & JIANG, C. (2000). Gating of inward rectifier K⁺ channels by proton-mediated interactions of N- and C-terminal domains. *Journal of Biological Chemistry* **275**, 31573–31580.

ROMERO, M. F., HEDIGER, M. A., BOULPAEP, E. L. & BORON, W. F. (1997). Expression cloning and characterization of a renal electrogenic Na$^+$/HCO$_3^-$ cotransporter. *Nature* **387**, 409–413.

ROMERO, M. F., HENRY, D., NELSON, S., HARTE, P. J., DILLON, A. K. & SCIORTINO, C. M. (2001). Cloning and characterization of a Na$^+$-driven anion exchanger (NDAE1). A new bicarbonate transporter. *Journal of Biological Chemistry* **275**, 24552–24559.

SCHULTE, U., HAHN, H., KONRAD, M., JECK, N., DERST, C., WILD, K., WEIDEMANN, S., RUPPERSBERG, J. P., FAKLER, B. & LUDWIG, J. (1999). pH gating of ROMK (K(ir)1.1) channels: control by an Arg–Lys–Arg triad disrupted in antenatal Bartter syndrome. *Proceedings of the National Academy of Sciences of the USA* **96**, 15298–15303.

SCHULTE, U., HAHN, H., WIESINGER, H., RUPPERSBERG, J. P. & FAKLER, B. (1998). pH-dependent gating of ROMK (Kir1.1) channels involves conformational changes in both N and C termini. *Journal of Biological Chemistry* **273**, 34575–34579.

SCHULTE, U., WEIDEMANN, S., LUDWIG, J., RUPPERSBERG, J. & FAKLER, B. (2001). K(+)-dependent gating of K(ir)1.1 channels is linked to pH gating through a conformational change in the pore. *Journal of Physiology* **534**, 49–58.

SCIORTINO, C. M. & ROMERO, M. F. (1999). Cation and voltage dependence of rat kidney electrogenic Na(+)-HCO(-)(3) cotransporter, rkNBC, expressed in oocytes. *American Journal of Physiology* **277**, F611–623.

SHYNG, S. L. & NICHOLS, C. G. (1998). Membrane phospholipid control of nucleotide sensitivity of K$_{ATP}$ channels. *Science* **282**, 1138–1141.

SIGWORTH, F. J. & SINE, S. M. (1987). Data transformations for improved display and fitting of single-channel dwell time histograms. *Biophysical Journal* **52**, 1047–1154.

SIMON, D. B., BINDRA, R. S., MANSFIELD, T. A., NELSON-WILLIAMS, C., MENDONCA, E., STONE, R., SCHURMAN, S., NAYIR, A., ALPAY, H., BAKKALOGLU, A., RODRIGUEZ-SORIANO, J., MORALES, J. M., SANJAD, S. A., TAYLOR, C. M., PILZ, D., BREM, A., TRACHTMAN, H., GRISWOLD, W., RICHARD, G. A., JOHN, E. & LIFTON, R. P. (1997). Mutations in the chloride channel gene, CLCNKB, cause Bartter's syndrome type III. *Nature Genetics* **17**, 171–118.

SIMON, D. B., KARET, F. E., HAMDAN, J. M., DIPIETRO, A., SANJAD, S. A. & LIFTON, R. P. (1996*a*). Bartter's syndrome, hypokalaemic alkalosis with hypercalciuria, is caused by mutations in the Na–K–2Cl cotransporter NKCC2. *Nature Genetics* **13**, 183–188.

SIMON, D. B., KARET, F. E., RODRIGUEZ-SORIANO, J., HAMDAN, J. H., DIPIETRO, A., SANJAD, S. A. & LIFTON, R. P. (1996*b*). Genetic heterogeneity of Bartter's syndrome revealed by mutations in the K$^+$ channel, ROMK. *Nature Genetics* **14**, 152–156.

TINKER, A., JAN, Y. N. & JAN, L. Y. (1996). Regions responsible for the assembly of inwardly rectifying potassium channels. *Cell* **87**, 857–868.

TSAI, T. D., SHUCK, M. E., THOMPSON, D. P., BIENKOWSKI, M. J. & LEE, K. S. (1995). Intracellular H$^+$ inhibits a cloned rat kidney outer medulla K$^+$ channel expressed in Xenopus oocytes. *American Journal of Physiology* **268**, C1173–1180.

TUCKER, S. J. & ASHCROFT, F. M. (1999). Mapping of the physical interaction between the intracellular domains of an inwardly rectifying potassium channel, Kir6.2. *Journal of Biological Chemistry* **274**, 33393–33397.

TUCKER, S. J., GRIBBLE, F. M., PROKS, P., TRAPP, S., RYDER, T. J., HAUG, T., REIMANN, F. & ASHCROFT, F. M. (1998). Molecular determinants of K$_{ATP}$ channel inhibition by ATP. *EMBO Journal* **17**, 3290–3296.

WANG, W., SCHWAB, A. & GIEBISCH, G. (1990). Regulation of small-conductance K channel in apical membrane of rat cortical collecting tubule. *American Journal of Physiology* **259**, F494–502.

WELLING, P. A. (1997). Primary structure and functional expression of of a cortical collecting duct Kir channel. *American Journal of Physiology* **273**, F825–836.

WIBLE, B. A., TAGLIALATELA, M., FICKER, E. & BROWN, A. M. (1994). Gating of inwardly rectifying K$^+$ channels localized to a single negatively charged residue. *Nature* **371**, 246–249.

WYSZYNSKI, M. & SHENG, M. (1999). Analysis of ion channel associated proteins. *Methods in Enzymology* **294**, 371–385.

XU, Z. C., YANG, Y. & HEBERT, S. C. (1996). Phosphorylation of the ATP-sensitive, inwardly rectifying K$^+$ channel, ROMK, by cyclic AMP-dependent protein kinase. *Journal of Biological Chemistry* **271**, 9313–9319.

YANG, J., JAN, Y. N. & JAN, L. Y. (1995). Control of rectification and permeation by residues in two distinct domains in an inward rectifier K$^+$ channel. *Neuron* **14**, 1047–1054.